A Geomorphology Based Approach for Digital Elevation Model Fusion - Case Study in Danang City, Vietnam

T. A. Tran[1], V. Raghavan[1], S. Masumoto[2], P. Vinayaraj[1], G. Yonezawa[1]

[1] Graduate School for Creative Cities, Osaka City University, Osaka, Japan.

[2] Graduate School of Science, Osaka City University, Osaka, Japan.

Correspondence to: T.A.Tran (tranthian.gis@gmail.com)

Abstract

Global Digital Elevation Model (DEM) is considered as vital spatial information and finds wide use in several applications. Advanced Spaceborne Thermal Emission and Reflection Radiometer (ASTER) Global DEM (GDEM) and Shuttle Radar Topographic Mission (SRTM) DEM offer almost global coverage and provide elevation data for geospatial analysis. However, GDEM and SRTM still contain some height errors that affect the quality of elevation data significantly. This study aims to examine methods to improve the resolution as well as accuracy of available free DEMs by data fusion technique and evaluating the results with high quality reference DEM. The DEM fusion method is based on the accuracy assessment of each global DEM and geomorphological characteristics of the study area. Land cover units were also considered to correct the elevation of GDEM and SRTM with respect to the bare earth surface. Weighted averaging method was used to fuse the input DEMs based on landform classification map. According to the landform types, the different weights were used for GDEM and SRTM. Finally, a denoising algorithm (Sun *et al.*, 2007) was applied to filter the output fused DEM. This fused DEM shows excellent correlation to the reference DEM having correlation coefficient R^2 = 0.9986 and the accuracy was also improved from Root Mean Square Error (RMSE) 14.9m in GDEM and 14.8m in SRTM into 11.6m in fused DEM.

1 Introduction

DEM is a digital model representing a surface which is presently used in many applications such as hydrology, geomorphology, geology and disaster risk mitigation. It is one of the essential inputs in modeling or simulating of landscape as well as dynamic natural phenomena such as flooding, soil erosion and landslide. Due to the important role of DEM in terrain related researches and applications, it is necessary to create high quality DEM at various levels of details. DEM can be generated using photogrammetry, interferometry, ground and laser surveying and other techniques (Mukherjee *et al.,* 2013). Usually, aerial photos, high resolution satellite data, or field surveyed spot height and Light Detection And Ranging (LiDAR) data are used as input to generate high resolution/high quality DEM. Surveying data collection is not only time consuming but also expensive. Even though a good number of aerial photos, high resolution Synthetic Aperture Radar (SAR) and optical remote sensing data are available, it is not always easy and affordable to generate DEM over large areas.

Recently, global free DEM including GDEM and SRTM offer almost global coverage and easily accessible data. These DEMs have been used in many applications, especially in geomorphology and hydrology (Zandbergen, 2008). However, GDEM and SRTM display some height errors, which affect the quality of elevation data significantly. Therefore, there have been several attempts to develop methodologies for enhancing quality of these global free DEMs.

Several authors (e.g. Li *et al.*, 2013, Ravibabu *et al.*, 2010, Zhao *et al.,* 2011, Suwandana *et al.*, 2012, Mukherjee *et al.,* 2013, Czubski *et al.*2013) have evaluated accuracy of GDEM as well as SRTM and carried out comparative evaluation of two DEMs. Results from these studies indicated that due to the inherent difficulties in acquiring satellite data both with the optical stereoscopic and the Interferometric Synthetic Aperture Radar (InSAR) technologies, global DEMs are not complete in themselves (Yang and Moon, 2003). Some authors (e.g. Reuter *et al.* 2007, Mukherjee *et al.,* 2013, Czubski *et al.*, 2013, Fuss, 2013) also evaluated the accuracy of global DEMs based on terrain characteristic. The vertical accuracy of these quasi-global DEMs varies depending on the terrain and land cover (Czubski *et al.,* 2013). The main purpose of these studies was to verify the quality of global DEMs. However the unique characteristics and different factors affecting the vertical accuracy of optical stereoscopy and InSAR provide an opportunity for DEM fusion (Kaab, 2005).

This study proposes a geomorphological approach for DEM fusion based on evaluation that the accuracy of GDEM and SRTM in mountain slopes, valleys and flat areas. This approach was used to combine DEM from different sources with appropriate weights to generate a fused elevation data. This could be an effective method to enhance the quality of global DEMs that have not been attempted in previous studies on DEM fusion (e.g. Kaab, 2005, Karkee *et al.*, 2008, Papasaika *et al,* 2011, Lucca., 2011, Fuss, 2013)

2 Study area

This study was conducted in Danang city in the Middle Central Vietnam (Fig. 1). The test site of 950 square km covers inland area of Danang city and is characterized by elevation ranging from 0m to 1664m a.m.s.l. Danang city is located on the Eastern Sea coast extend from $15^0$55'N to $16^0$14'N and $107^0$18'E to $108^0$20'E. The topography of this area has great variation from flat to mountainous region. Due to varying of topography and geomorphology, the optical stereoscopy technique used to generate GDEM as well as InSAR technique used in SRTM show different representation on DEM data, and contain inherent anomalies that need to be detected and minimized.

There are few studies in this area using global free DEMs such as GDEM or SRTM. Ho *et al.* (2011, 2013) developed a landform classification method and flood hazard assessment of the Thu Bon alluvial plain, central Vietnam. In their study, the authors used SRTM as an input DEM source and applied bias elimination method to correct surface elevation data to the height of bare-earth surface. However, SRTM with low resolution (90m) may not give sufficient terrain information. Also, InSAR technique used in SRTM may fail to provide reliable estimate elevation if images contain layovers, non-linear distortion of the images due to slanted geometry of the radar sensing and shadows, or suffer from temporal decorrelation and changes in atmospheric conditions between two acquisitions (Karkee *et al.*, 2008). Although Ho *et al.*(2013) already masked the high and upland areas and focused only on a low-lying alluvial plain, their research did not discuss about methods to enhance accuracy of free DEM, especially in the areas that have high topographic relief.

3 DEM datasets

The global free DEMs used in this study include GDEM Version 2 (http://earthexplorer.usgs.gov) and SRTM Version 4.1 (http://www.cgiar-csi.org). GDEM Version 2 released on October 2011 has the resolution of 30m. GDEM data was compiled from over 1.2 million scene-based DEMs covering land surface between 83^0N and 83^0S latitudes. GDEM was generated from ASTER optical satellite images using stereoscopy technique with differ look angles of sensor. The Terra spacecraft used in ASTER GDEM is capable of collecting in-track stereo using nadir- and aft-looking near infrared cameras (ASTER GDEM validation Team, 2011). DEM from such optical satellite images as GDEM usually contains some height errors because of cloud coverage. ASTER GDEM Version 2 was improved with respect to Version 1 (released on June 2009) due to better data processing algorithm and additional data used during the processing. However, the revised version still contains anomalies and artifacts which are needed to be corrected before using in any application, especially on a local scale (ASTER GDEM validation Team, 2011)

SRTM Version 4.1 has been obtained from the Consortium for Spatial Information (CGIAR-CSI; http://www.cgiar-csi.org). The DEM data was derived from 11 days Shuttle Radar Topographic Mission flew in February 2000, and has provided publicly available elevation surface data for approximately 80 percent (from 60^0 N to 56^0 S) of the world land surface area (Reuter *et al.*, 2007). The SRTM elevation data are derived from X-band and C-band Interferometric Synthetic Aperture Radar (InSAR) sensor. The first release of SRTM was provided in 1-degree DEM tiles in 2003. When the data was processed by NASA and the USGS, it was made available at 1-arc second resolution (approximately 30m) for the United

States, and 3-arc second resolution (approximately 90m) for the rest of the world. The Consortium for Spatial Information of the CGIAR (CGIAR-CSI) is offering post-processed 3-arc second DEM data for the globe. The original SRTM has been subjected to a number of processing steps to provide seamless and complete elevation surface for the globe. In its original release, SRTM data contained regions of no-data, specifically over water bodies (lakes and rivers), and in areas where insufficient textural detail was available in the original radar images to produce three-dimensional elevation data (http://www.cgiar-csi.org). Presently, the latest version of SRTM released by CGIAR-CSI is SRTM Version 4.1. SRTM V4.1 has some advantages than previous versions such as filling void areas and masking water bodies. SRTM was used in this study has the resolution of 90m. Although SRTM has lower resolution than GDEM, it offers coverage in all weather conditions since it uses InSAR technique. However, because of the limitation of resolution and vertical error in some areas, SRTM need to be edited before using in any application. Both GDEM and SRTM are in geographic coordinate system, with the WGS84 horizontal datum and the EGM96 vertical datum.

Reference elevation data used in this study is a DEM generated from the 1:10,000 topographic map of Danang city published in 2010, including contour lines with 5m interval and spot heights elevation data developed by Department of Natural Resource and Environment (DONRE), Danang city, Vietnam. Contour lines were derived from aerial photos of Danang city captured on 2003, and additionally surveyed and modified during 2009. Spot heights elevation data were surveyed in 2009. The data are projected in a Vietnamese projection named VN2000. In this study, the DEM generated from contour and spot heights elevation is referred to as the "reference" DEM. Firstly a DEM was generated from contour map using Regularized Spline with Tension (RST) algorithm. The RST interpolation is considered as one of the effective interpolation methods available for elevation data (Hofierka *et al.*, 2002). RST method is based on the assumption that the approximation function should pass as closely as possible to the given data and should be as smooth as possible (Mitasova *et* *al.*, 1995). RST interpolation was carried out in GRASS GIS open source software (http://grass.osgeo.org). However, the contour lines do not cover the whole area of Danang city. In flat area with elevation less than 10m, there are no contour lines. Large number of spot heights data is available for flat area (more than 190,000 elevation points) and Inverse Distance Weighting (IDW) interpolation was applied to generate the DEM where contour data are not available and merged with DEM generated using RST with contour data for hilly area. This reference DEM was also generated at resolution of 30m. The RMSE of reference DEM comparing to spot heights data is 1.66m. Some statistical data on global DEMs and reference DEM is shown in Table 1. The mean elevation and standard deviation (STD) in GDEM and SRTM are analogous to reference DEM. Due to some artifacts located on GDEM, maximum elevation value of GDEM (8016m) shows significant dissimilarity. Compare to GDEM, STD of SRTM (304.6m) is almost similar to reference DEM (302.6m).

4 Methodology

SRTM was re-interpolated from 90m to 30m resolution in order to compare with other DEM at same resolution. The artifacts in GDEM were eliminated using fill and feather method (Dowding *et al.*, 2004). DEM alignment was also carried out in order to co-register GDEM and interpolated SRTM with respect to reference DEM. Next, both GDEM and SRTM were evaluated in term of vertical and horizontal accuracy. The quality of each DEM was also assessed according to different topographic conditions. The result of evaluation has been used to devise an appropriate DEM fusion method considering various factors responsible for degradation of data quality. Basically, there is a difference between the Digital Surface Model (DSM) like GDEM, SRTM and the Digital Terrain Model (DTM) that refers to the bare-earth surface. The overestimations as well as underestimated elevation values in GDEM and SRTM need to be detected and corrected by comparing these elevation data to reference DEM on the basis of geomorphology and land cover map. In the case of land cover category, the offsets were calculated by taking mean values of the difference in elevation between global DEMs and reference DEM. The corrected GDEM and SRTM were used as input data for DEM fusion process. Landform classification map was generated from SRTM to determine the area suitable for different fusion methods. The algorithm used in DEM fusion process is weighted averaging based on geomorphologic characteristics. In relatively flat areas, the higher weight was used for SRTM and lower weights for GDEM. In the mountainous areas, SRTM and GDEM were weighted equally. The higher weight was applied for GDEM in the valley areas, because of the limitation of SRTM in those areas. The output fused DEM was filtered using denoising algorithm according to Sun *et al.,* 2007. Finally, fused DEM was compared to reference DEM to assess the efficiency of DEM fusion method.

The data processing described above is shown in Fig. 2. The data fusion workflow includes four main steps, namely pre-processing, DEM quality assessment, bias elimination and DEM fusion.

4.1 Pre-processing

It is observed that SRTM has anomalies in the coastal area and some small areas inland with negative values. 377 pixels show negative values and cover about 0.34 square kilometer area. These pixels were filled by averaging elevation of 3 by 3 neighboring pixels. SRTM and GDEM have been converted from geographic coordinates to UTM_WGS84_zone 49N projection. Reference DEM was also converted from VN2000 to UTM_WGS84_zone 49N projection. The vertical datums used in Global DEMs and reference DEM are different. Global DEMs use EGM96 vertical datum, while reference DEM uses Vietnamese vertical datum named Hon Dau_Hai Phong, that is related to m.s.l in Hon Dau island, Hai Phong province, Vietnam. An offset 1.5m downwards was applied to convert Global DEMs from EGM96 to Hon Dau_Hai Phong vertical datum.

SRTM was interpolated from 90m to 30m using RST algorithm, which is available in GRASS GIS as *r.resamp.rst* function. RST interpolation not only re-samples the DEM to higher resolution but also reduces the staircase effect in the original SRTM and smoothen the

DEM surface. Fig. 5a and Fig. 5b show the profile of SRTM compared to reference DEM before and after interpolation. The interpolated SRTM also has better RMSE and correlation to reference DEM than the original 90m data (Table 3).

GDEM has some artifacts in the western mountain part of Danang city, with extreme high elevation values. These artifacts may be caused due to cloud coverage that is very common in optical satellite data. These artifacts are the main reason for high RMSE (75.6m) observed in raw GDEM (Table 2). The artefacts in GDEM need to be eliminated before further processing. Several algorithms for voids filling have been proposed such as kriging, spline, IDW (Reuter *et al.*, 2007), moving window (Karkee *et al.*, 2008), fill and feather (Dowding *et al.* 2004), delta surface fill (Grohman 2006). All the void filling algorithms can be categorized into three groups namely interpolation, moving window and fill and feather (F&F). F&F method proposed by Dowding *et al.* (2004) was applied in this study to fill artifacts in GDEM. In the F&F approach, an artefact is replaced with the most accurate digital elevation source available with the void-specific perimeter bias removed (Grohman, 2006). The artifacts were detected by overlaying the slope map of GDEM and the difference elevation map between GDEM and reference DEM, and digitizing from the anomalies that can be visualized from the overlaying display. SRTM was chosen as an auxiliary data to fill the artifacts for GDEM. After filling these artifacts, the surface will be feathered to mitigate any abrupt change (Grohman, 2006). In this case study, DEM surface will be feathered in the final step of data processing using filtering algorithm. As the result, GDEM after filling artifacts has the RMSE error only 14.9m. The scatter plot of GDEM after filling also shows the good correlation to reference DEM, while the original one has a several outliers (Fig. 3). Comparing to original GDEM, it can also be seen that most of the artifacts were eliminated.

4.2 DEM quality assessment

The horizontal accuracy of the global DEMs was evaluated by comparing the extracted stream networks (Fig. 4). Stream networks extracted from reference DEM, GDEM and SRTM indicate that SRTM has a horizontal difference about 15m, and GDEM has difference around 30m with respect to reference DEM. Therefore, GDEM was shifted one pixel to the east, and SRTM was shifted half pixel to the west, in order to align all input DEMs before fusion process. Fig. 5 compares the profiles of GDEM, SRTM and reference DEM before and after shifting. The ridge lines as well as canyon bottoms in GDEM and SRTM become more similar with reference DEM. In Table 2, GDEM after shifting shows better RMSE and correlation with reference DEM as compared to before shifting.

In this study area, RMSE of GDEM and SRTM with respect to reference DEM observed as 14.9m and 14.8m respectively (Table 2 and Table 3). The correlation coefficient (R^2) of GDEM in the whole area is 0.9976 while this value in original SRTM is 0.9979. The accuracy of the individual DEM should be considered based on different topographic condition. Figure 6 shows the correlation coefficients of each global DEM in flat and mountain area. In mountain area, GDEM and SRTM have the similar correlation with reference DEM (0.9966 and 0.9969, Fig. 6b). However, in some specific areas, especially in the steep valleys, GDEM provides better accuracy than SRTM. The circled areas in Fig. 5 show that GDEM preserves the considerable details of topography in the valley areas, while SRTM is ineffective in those areas. In such valley areas, SRTM seems to suffer from layover and shadow effects. In the case of a very steep slope, targets in the valley have a larger slant range than related mountain tops, consequently the fore-slopes are "reversed" in the slant range image. This is referred to as layover effect when the ordering of surface elements on the radar image is the opposite of the ordering on the ground (European Space Agency, https://earth.esa.int/applications/data_util/SARDOCS/spaceborne/Radar_Courses/Radar_Course_III/layover.htm). Radar shadow is caused when a slope is away from the radar illumination with an angle that is steeper than the sensor depression angle (European Space Agency, https://earth.esa.int/applications/data_util/SARDOCS/spaceborne/Radar_Courses/Radar_Course_III/shadow.htm). In such areas, SRTM may not provide sufficient information, compared to GDEM or other

DEM sources. In relatively flat areas, the correlation coefficient between SRTM and reference DEM (R^2=0.8504) is better than GDEM (R^2=0.5578) (Fig. 6a). This is because degradation of elevation estimate of GDEM in the area has low topographic relief. In the profile of Fig. 7, it can be seen that GDEM has many spikes and unstable elevation values in this flat area, while SRTM shows similar trends as the reference DEM.

The difference elevation maps of global DEMs were also generated by subtracting GDEM and SRTM values to reference DEM. Both GDEM and SRTM show high vertical error in mountain area, and lower vertical error at flat area (Fig. 8). These errors occur because of the forest cover in mountain area and due to some limitations of the sensing techniques used to generate DEM in high relief area. The profile of SRTM from the difference elevation map in flat area is closer to 0m line (Fig.8), while GDEM contains higher difference and spikes that affect the quality of GDEM significantly.

4.3 Minimizing DEM bias effect

The topographic height variation between global DEMs and reference DEMs is caused due to the differences in vertical datum used and in primary data collection methods. Vertical datum is one of the reasons for difference in elevation between global DEMs and reference DEM. In addition, both GDEM and SRTM that were generated from satellite data are DSM, while reference DEM considered as bare earth DTM, this difference also introduces the bias offsets depending on the land cover.

Firstly, global DEMs were converted to Hon Dau_Hai Phong vertical datum. According to Vietnam Land Administration, the global EGM96 model is almost similar to the Vietnamese vertical datum, 97% of data shows the height difference around 1.5m, only 3% of data shows higher than 1.5m (Nguyen and Le, 2002). Therefore, an offset of 1.5m was subtracted from global DEMs considering height difference between EGM96 and Vietnamese vertical datum.

Secondly, the height offsets of global DEMs were determined based on land cover map. Because the SRTM data was derived in 2000 and GDEM data was collected from millions of

ASTER imagery from 1999 to 2009, a land cover map of Danang city in 2001 were used to calculate the height offsets for global DEMs. These offsets were calculated based on the difference elevation maps of GDEM and SRTM with respect to reference DEM considering land cover. This was done using *r.statistics* function in GRASS GIS. The mean elevation differences on each land cover type were calculated, and used as offsets to verify elevation for GDEM and SRTM (Table 4). As the result, GDEM has the highest difference in the water body (4m). This error is common in GDEM because water surface give very low reflectance value in optical satellite data. The elevation value of GDEM in bare land is underestimated (-2m) with average 2m lower than reference DEM. These bare land surfaces are located in flat area where the topographic relief is inadequate for optical stereoscopy technique. GDEM in such areas can, therefore, not provide reliable elevation information. In SRTM, the highest error is observed in forest land cover type (6.3m) which mostly cover mountainous areas. SRTM in mountainous areas revealed relatively higher errors, because layovers and shadows effect on the quality of radar data. The significant error in SRTM is also observed in bare land area (3.8m). The scattering energy back from bare land is too small to create a radar image. From global assessment of the SRTM data, voids were found to be very common in mountainous areas, as well as in very flat areas especially in deserts (Zandbergen, 2008). SRTM V4 used in this study already dealt with water body problem using a number of interpolations techniques and void filling algorithms (Reuter *et al.*, 2007). Therefore, the error of SRTM in water bodies currently is only 0.4m (Table 4).

Based on the above investigations, the elevation for GDEM and SRTM with respect to reference DEM were corrected by subtracting GDEM and SRTM to the elevation offsets for each land cover type (Table 4). The calculation was executed by *r.mapcalc* function in GRASS GIS software using land cover map as the base. The corrected GDEM and SRTM were used as input data for DEM fusion processing.

After removing the offsets, GDEM and SRTM were compared to reference DEM again to make better input for DEM fusion processing. The mean value of GDEM and SRTM with respect to each elevation value in reference DEM was calculated. Fig.9a shows the behavior of global DEMs with respect to reference DEM, from flat to mountainous area. In the A and C area (Figure 9b and Figure 9d), the mean elevation of SRTM is closer to reference DEM, while the profile of GDEM shows higher error. In case of B area (Figure 9c), both SRTM and GDEM show the good correlation to reference DEM. In Figure 9e, the profile of GDEM is comparable to reference DEM in this mountainous area. From this analysis, it is evident that using a global data fusion for the whole area is not a good solution. Appropriate weights for DEM fusion process need to be considered depending upon the topographic context, and is used as the basis for DEM fusion in this study.

4.4 DEM fusion algorithm

Both GDEM and SRTM contain intrinsic errors due to primary data acquisition technology and processing methodology in relation with a particular terrain and land cover type (Mukherjee *et al,* 2013). The optical stereoscopy technique used in GDEM is limited by the cloud coverage, radiometric variation and low levels of texture (Karkee *et al.,* 2008) while InSAR technique used in SRTM may not work well in case of shadowing, layovers or complex dielectric constant (Reuter *et al.,* 2007). Combination of two data can take into account the advantages of each DEM source and provide complimentary inputs to enhance the quality for the global DEMs. DEM fusion workflow combines weighted averaging and denoising algorithm (Sun *et al,* 2007).

4.4.1 Weighted Averaging

Several authors have proposed fusion methods for digital elevation data. Karkee *et al.* (2008) carried out a fusion between GDEM and SRTM using Fast Fourier Transformation (FFT) combining with frequency domain filtering. Papasaika *et al*. (2011) has proposed an approach that performs DEM fusion using sparse representations. Lucca (2011) examined different DEM fusion methods, such as weighted averaging and collocation prediction, and compared the result to LiDAR DSM to assess the improvement of DEM fusion. Fuss (2013) has developed a DEM fusion algorithm from multiple, overlapping DEMs, using slope thresholding, K-means clustering and filtering of elevations. Tran *et al.* (2013a and 2013b) has given a fusion method by selecting appropriate DEM source based geomorphological conditions. The most frequent DEM fusion method that has been suggested is weighted averaging. The weighted mean ($\overline{x}$) of a non-empty set of data {x_1, x_2,...,x_n} with non-negative weights{ω_1,ω_2,...,ω_n} (Papasaika, 2012) is shown:

$$\overline{x} = \frac{\sum_{i=1}^{n} \omega_i x_i}{\sum_{i=1}^{n} \omega_i} = \frac{\omega_1 x_1 + \omega_2 x_2 + \cdots + \omega_n x_n}{\omega_1 + \omega_2 + \cdots + \omega_n} \qquad (1)$$

Where: x_1,x_2,...,x_n are the input DEMs.

ω_1,ω_2,...,ω_n are the weights for DEM fusion.

However, weighted averaging applied in previous studies referred in the earlier section consider weights based on the accuracy of the whole raster DEM source. Each raster DEM (x_1,x_2,...,x_n) is used as one input data for weighted averaging. Actually, the DEM accuracy also changes depends upon the topographic context. Therefore, in this research, a new method for DEM fusion using weighted averaging based on geomorphologic characteristics was proposed. Firstly, a landform map was extracted from SRTM. This landform classification method was done according to Dickson and Beier (2006). The algorithm is based on Topographic Position Index (TPI) and slope map. In general, TPI allows to classify landscape into discrete landform categories by comparison of individual cell heights with an average height of neighboring cells (Czubski *et al.*, 2013). TPI based landform classification method according to Dickson and Beier (2006) can be denoted as below:

Valley : TPI<= -8

Flat : -8 < TPI <= 8, slope < 6^0

Steep slope : -8 < TPI <= 8, slope >= 6^0

Ridge line : TPI > 8

In this study, three categories demarcated from the landforms classification result, namely, mountain slopes (include ridge lines and steep slopes), valleys, and flat areas (Fig. 10).

In order to determine the weight for global DEM on each landform class, the following equation (Hengl and Reuter, 2009) was applied:

$$w_i = \frac{1}{a^2} \qquad (2)$$

Where w_i is the weight for each DEM source for a given landform unit.

"a" is given accuracy parameter for the DEM for a given landform unit.

Terrain related parameters were used to determine weighting scheme for DEM fusion. Firstly, slope error (difference in slope between global DEMs and reference DEM) was use to compare the accuracy of GDEM and SRTM on flat, valley and mountain slope areas. On each landform area, the mean of absolute error (MAE) from slope error map was calculated. The result can be shown in Table 6.

In flat area, GDEM has many overestimates and unstable elevation values. Therefore slope error of GDEM is larger than SRTM in this area. The weight used for GDEM can be determined according to equation (2): $w_1 = 1/(2.1)^2 = 0.22$, and the weight for SRTM can be shown as: $w_2 = 1/(1.6)^2 = 0.39$. It can be seen that $w_2 \approx 2*w_1$, therefore the following formula was applied for DEM fusion in flat area:

$$\text{Fused DEM} = (\text{GDEM} + \text{SRTM}*2)/3 \qquad (3)$$

In mountain slope area, the similar way was applied to calculate weight for DEM fusion, using MAE of slope error. In this case, GDEM and SRTM have almost same MAE (6.08 and 6.1 degree). Therefore, the same weights were applied for GDEM and SRTM in steep slope area ($w_1 = w_2$). The following equation was used in mountain slope is:

$$\text{Fused DEM} = (\text{GDEM} + \text{SRTM})/2 \qquad (4)$$

In valley, GDEM and SRTM also have the similar MAE of slope error (5.8 and 5.7 degree). However, considering the topographic characteristic in some steep valleys, it can be seen that SRTM is ineffective in representing valley bottom, while GDEM is still more correlative to reference DEM (Fig. 5). In case of valley landform, Slope Variability (SV) (Popit and Verbovsek, 2013) was used to determine weight for DEM fusion. SV was calculated by the distance between maximum and minimum slope in a neighborhood of 3 by 3 pixels. SV error of GDEM and SRTM with respect to reference DEM were calculated. GDEM has MAE of SV error about 5.6, and SRTM has an error about 7.3 degree. The weight for GDEM was calculated according to formula (2): $w_1 = 1/(5.6)^2 = 0.032$, and the weight for SRTM is as: $w_2 = 1/(7.3)^2 = 0.018$. It can be observed that $w_1 \approx 2*w_2$, therefore the following formula was used for DEM fusion in valley:

$$\text{Fused DEM} = (\text{GDEM}*2+\text{SRTM})/3 \qquad (5)$$

The weighted averaging method based on landform classification map is shown in Fig.11.

4.4.2 Filtering the noises for fused DEM

The fusion of different DEMs involves the problem, since the DEMs obtained from different sources and have different resolutions as well as accuracies (Lucca, 2011). The bias elimination for GDEM and SRTM also use different offsets depending up on the land cover. Different weights have been used for DEM fusion in each landform type. Therefore, it is essential to filter the fusion DEM to reduce the mismatched and noisy data. In this study, denoising algorithm (Sun *et al.*, 2007) was used to minimize the noise effect. The level of denoising is controlled by two parameters, namely, the threshold (T) that controls the sharpness of the features to be preserved, and the number of iterations (n) that controls how much the data are smoothed. The optimum settings depend up on the nature of the topography and of the noise to be removed (Stevenson *et al.,* 2009). The Sun's algorithm (Sun *et al.*,2007) has been implemented in GRASS GIS as an add-on (*r.denoise*). In this denoising process, the topographic feature need to be preserved as far as possible in the fused DEM, so the parameters that were used are $T = 0.95$ and $n = 5$. As the result, fused DEM becomes more smooth and the mismatched surfaces are minimized. The profile of fused DEM is also very much comparable to the reference DEM (Fig. 12).

5. Results and discussions

Weighted averaging based on landform classification map has been verified as an effective method for DEM fusion. The accuracy of fused DEM can be evaluated by statistical analysis such as RMSE, MAE and linear regression. The MAE and RMSE of fused DEM was much improved compared to available global DEMs. The RMSE was reduced from 75.6m in original GDEM, 14.9m in GDEM after removing artifacts and 13m in GDEM after bias elimination to 11m in fused DEM. In SRTM, the RMSE was reduced from 14.8m in original SRTM, and 11.4m in processed SRTM into 11m in fused DEM (Table 5).

The linear regression between fused DEM and reference DEM also shows the significant correlation between two DEMs with R^2 = 0.9986 (Figure 13). Comparing to original data with correlation coefficient for GDEM and SRTM are 0.9976 and 0.9979 respectively, it can be, therefore, concluded that fused DEM show better correlation with the reference DEM.

Statistical comparison of vertical accuracy of GDEM, SRTM and fused DEM is shown in Table 5. The minimum error, maximum error, MAE, and RMSE of fused DEM show improvement when compared with GDEM and SRTM before fusion. Due to the smoothing, the final fused DEM shows a slight increase in RMSE in comparison with fused DEM before denoising. The final fused DEM can minimize the mismatched surface and afford better extraction of topographic parameters. Based on the difference elevation map of fused DEM (Fig. 14), it can be seen that the height error in fused DEM is also greater in mountainous area, especially in steep slope area. The minimum amount of error was observed in relatively flat area. Figure 15 shows the histogram from the difference elevation maps of SRTM, GDEM and fused DEM with respect to reference DEM. In the fused DEM, the center of histogram reach to value of 0m difference, and the number of cells have lowest difference (0m) are also most frequent. This result reveals that there is significant improvement in quality of global DEMs using the proposed DEM fusion algorithm.

The slope, profile curvature and tangential curvature maps were extracted from GDEM, SRTM and fused DEM. Then the error maps with respect to reference DEM were created in each terrain parameter (Table 7). Comparing to GDEM and SRTM, fused DEM has smaller MAE, STD and the better correlation with reference DEM. Figure 16 shows the slope, profile curvature and tangential curvature maps from fused DEM. In these DEM derivative parameters, no major anomaly or terrace artifacts can be seen in the transition zones between landform classes.

Aspect is calculated as circular degrees clockwise from 0° to 360°, and it is therefore difficult to compare quantitatively (Deng *et al.*, 2007). In order to assess the accuracy in aspect as well as slope, unit Normal Vector (NV) of topographic surface was considered. The NV of global DEMs and fused DEM were computed from slope and aspect values of respective DEM. The NV from these DEMs then were compared with reference DEM to determine the angular difference between two NVs (Figure 17). The NV of the terrain surface ($\vec{T}$) can be calculated as below as suggested by Hodgson and Gaile (1999).

$$\vec{T} = [x, y, z] \quad (6)$$

Where

x = sin(aspect)*sin(slope)

y = cos(aspect)*sin(slope)

z = cos(slope)

To derive the three-dimensional angular difference between two unit NVs pointing away from the same origin, the following formula was applied:

$$\cos(i) = \vec{T} * \vec{S} = t_x*s_x + t_y*s_y + t_z*s_z \quad (7)$$

The result of angular differences of NV is shown in Table 8. As a result, fused DEM has smaller mean error than GDEM and SRTM, and STD of fused DEM are also comparable with global DEMs.

The Topographic Roughness Index (TRI) was also considered to assess the quality of fused DEM. In this study, TRI was used as amount of elevation difference among the adjacent cells of a DEM (Mukherjee *et al*, 2013). The residuals in elevation between a grid cell and its eight neighbors were derived, and the RMS of the elevation differences was calculated as TRI. The TRI of reference DEM and GDEM, SRTM and fused DEM show correlation coefficient of 0.71, 0.75 and 0.76 respectively (Table 7). The TRI derived from fused DEM compare well with the reference DEM as compared with GDEM and SRTM.

6. Conclusions

Global free DEMs generated from remote sensing data always have some vertical and horizontal errors. Assessing the quality of global DEMs and validating their accuracy before using in any application is very important. In this study, the accuracy of GDEM and SRTM were determined based on height differences with reference DEM. The artifacts with extreme high elevation values in GDEM were eliminated by using SRTM as an auxiliary data. River networks extracted from both DEMs that were used to detect and correct the horizontal errors for global DEMs can make better co-registration. The bias effect caused by tree-top canopy and building on global DEMs was also calculated by comparing these DSMs with the elevation from reference DEM. A land cover map of Danang city in 2001 was used to calculate the height difference of GDEM and SRTM on each land cover type. Once the bias offsets were determined, effort was made to correct the elevation of these DEMs with respect to the bare land surface.

Based on global DEMs assessment in Danang city, it is observed that the accuracy of GDEM and SRTM varies depending upon the geomorphological characteristics of target area. Fusion between two global DEMs using geomorphological approach is an appropriate solution to enhance the quality of free DEMs for Danang city, Vietnam. The data fusion technique was applied by weighted averaging of GDEM and SRTM based on the topographic context. The weighting scheme was determined according accuracy parameters including MAE of slope and slope variability. The weights used for each DEM were changed locally according to the landform types. The results were compared with reference DEM to discuss about accuracy and impact of landform in variation on DEM quality. Terrain related parameters such as slope, curvature, TRI and NV of topographic surface were considered to assess seriously the quality of fused DEM. Results indicate that the fused DEM has improved accuracy than individual global DEM and most artifacts are successfully eliminated. The proposed method supports the effective utilization for the areas where the better quality DEM is not available.

In future work, the more robust weighting scheme needs to be considered by defining more number of landform types. In this regard, the landform classification method may also need to be improved further. In future, we plan to investigate landform classification using *r.geomorphon*, a new add-on that is available in GRASS 7. A “geomorphon” is a relief-invariant, orientation-invariant, and size-flexible abstracted elementary unit of terrain (Stepinski *et al.,* 2011). This landform classification map will, not only be good way to compare the height errors in micro-geomorphological classes, but also help to compare terrain parameters extracted from fused global DEMs and reference DEM.

The difference in elevation between DEM and DSM are useful for estimating the canopy height especially in areas used for sylviculture. Further investigation on bias effect introduced by land cover and sylviculture needs to be carried out. The relationship between land cover and geomorphology also need be studied in future, to understand the impact of topographic condition on land cover change. Several new satellite data including ALOS-2 PRISM and PALSAR-2 (http://www.eorc.jaxa.jp/ALOS/en/index.htm) need to be incorporated to enhance the methods for multi-resolution DEM fusion based on a better understanding of characterises of DEM derived from multiple sources.

*Acknowledgements.*This study was conducted under the Mobukagakusho (MEXT) scholarship that supported by Japanese government. We sincerely thank to MEXT and Osaka City University for the financial and facilities support for our research. We are also grateful to Department of Natural Resource and Environment, Danang City, Vietnam for supporting the reference data. The authors would like to express a sincere gratitude to Prof. Xianfeng Song, Graduate University of Chinese Academy of Science who has given us a lot of valuable comments on geomorphological analysis. We also sincerely thank to Dr. Susumu Nonogaki, National Institute of Advanced Industrial Science and Technology (AIST), Japan, for his kind help on DEM generation. The authors also thank to Dr. David Hastings for his critical comments that helped in improving the quality of this paper.

References

Arefi, H. and Peter, R.: Accuracy Enhancement of ASTER global digital elevation models using ICESat data, Remote Sens.,3,1323-1343, doi:10.3390/rs3071323,2011.

ASTER GDEM Validation Team: ASTER global DEM validation summary report, June 2009.

ASTER GDEM Validation Team: Advanced Spaceborne Thermal Emission and Reflection Radiometer (ASTER) Global digital elevation model (GDEM) Version 2, October 2011.

Crosetto, M. and Crippa, B.: Optical and Radar fusion for DEM generation, IAPRS, Vol.32, Part 4, ISPRS Commission IV Symposium on GIS - Between Vision and Applications, Stuttgart, Germany, 128-134,1998.

Czubski, K., Kozak, J., and Kolecka, N.: Accuracy of SRTM-X and ASTER elevation data and its influence on topographical and hydrological modeling: case study of the Pieniny Mts. in Poland, International Journal of Geoinformatics, 9, 7 - 14,2013.

Deng, Y., Wilson, J.P. and Bauer, B.O.: DEM resolution dependencies of terrain attributes across a landscape, Int. J. Geographical Information Science, 21:2, 187-213, doi: 10.1080/ 13658810600894364, 2007.

Dickson, B.G. and Beier, P.: Quantifying the influence of topographic position on cougar (Puma concolor) movement in southern Califonia, USA, Journal of Zoology, 271, 270-277, 2006.

Dowding, S., Kuuskivi, T., and Li, X.: Void fill of SRTM elevation data-Principles, processes, and performance, Images to decisions: Remote sensing foundations for GIS applications, ASPRS 2004 Fall conference, Kansas city, MO, USA,2004.

Fuss, C.E.: Digital elevation model generation and fusion, Master thesis in Geography, University of Guelph, Ontario, Canada, 2013.

Grohman, G., Kroenung, G., and Strebeck, J.: Filling SRTM voids: the delta surface fill method, Photogramm. Eng. and Rem. S., 72, 213 - 216, 2006.

Hengl, T. and Hannes I. R.: Geomorphometry, Concept, Software, Applications, Elsevier-Development in Soil science,33, 111, 2009.

Ho, T.K.L. and Umitsu M.: Micro-landform classification and flood hazard assessment of the Thu Bon alluvial plain, central Vietnam via an integrated method utilizing remotely sensed data, Appl. Geogr., 31, 1082-1093, 2011.

Ho, T.K.L, Yamaguchi, Y., and Umitsu M.: Rule-based landform classification by combining multi-spectral/temporal satellite data and the SRTM DEM, International Journal of Geoinformatics, 8, 27-38,2013.

Hodgson, M. E. and Gaile., L.: A cartographic modeling approach for surface orientation-related applications, Photogramm. Eng. Rem. S., 65:1, 85-95, 1999.

Hofierka, J., Parajka, J., Mitasova, H., and Mitas, L.: Multivariate interpolation of precipitation using regularized spline with tension, Transactions in GIS, 6,135-150, 2002.

Kaab, A.: Combination of SRTM3 and repeat ASTER data for deriving alpine glacier flow velocities in the Bhutan Himalaya, Remote Sens. Environ., 94, 463-474, 2005.

Karkee, M., Steward, B. L., and Aziz, S. A.: Improving quality of public domain digital elevation models through data fusion, Biosyst. Eng., 101, 2008, 293 - 305,2008.

Li, P., Shi, C., Li, Z., Muller, J., Drummond, J., Li., X., Li, T., Li, Y., and Liu, J.: Evaluation of ASTER GDEM using GPS bechmarks and SRTM in China, Int. J. Remote Sens., 34, 1744-1771,2013.

Lucca, S.: Validation and fusion of digital surface models, PhD. thesis, Ph.D. Course in Environmental and Infrastructure Engineering, Department of Environmental, Hydraulic, Infracstructure and Surveying Engineering, Polytechnic University of Milan, Italy, 2011.

Mitasova, H., Mitas, L., Brown, W. M., Gerdes, D.P., Kosinovsky, I., and Baker, T.: Modeling spatially and temporally distributed phenomena: new methods and tools for GRASS GIS, Int. J. Geogr. Inf. Syst., 9, 433-446, doi:10.1080/ 02693799508902048, 1995.

Mukherjee, S., Joshi, P.K., Mukherjee, S., and Ghosh, A.: Evaluation of vertical accuracy of open source digital elevation model (DEM), Int. J. Appl. Earth Obs., 21, 205-217, 2013.

Mukherjee, S., Mukherjee, S., Garg, R.D., Bhardwaj, A and Raju, P.L.N.: Evaluation of topographic index in relation to terrain roughness and DEM grid spacing, J. Earth Syst. Sci., 122-3, 869-886, 2013.

Nguyen, L.N and Le, H.V: Methods for positioning ellipsoid over the Vietnam area based on EGM96 model, Ho Chi Minh University of Technology, Vietnam, 1 - 9, 2002.

Papasaika, H., Kokiopoulou, E., Baltsavias, E., Schindler, K., and Kressner, D.: Fusion of digital elevation models using sparse representation, Photogrammetric Image Analysis, Lect. Notes Comput. Sc., 6952, 171-184, doi:10.1007/978-3-642-24393-6-15, 2011.

Popit, T and Verbovsek, T.: Analysis of surface roughness in the Sveta Magdalena paleo-landslide in the Rebrnice area, RMZ_M&G, 60, 197-204, 2013.

Reuter, H.I., Nelson, A., and Jarvis, A.: An evaluation of filling interpolation methods for SRTM, Int. J. Geogr. Inf. Sc., 21, 983-1008, 2007.

Ravibabu, M., Jain, K., Singh, S., and Meeniga, N.: Accuracy improvement of ASTER stereo satellite generated DEM using texture filter, Geo-spatial Information Science, 13, 257-262, 2010.

Stepinski, T. F. and Jasiewicz, J.: Geomorphons- a new approach to classification of landforms, Geomorphometry.org/2011, 7-11 September, Redlands, CA,109 - 112, 2011.

Stevenson, J. A., Sun, X., and Mitchell, N. C.: Despeckling SRTM and other topographic data with a denoising algorithm, Geomorphology, 114, 238 - 252, doi:10.1016/j.geomorph.2009.07.006, 2009.

Stevesok, Muller, J.P., and Morley, J.: Investigation into different DEM fusion methods for creation of a global uniform 30m DEM based on ASTER GDEM and SRTM and other sources, Msc Poster fair, Department of Civil, Environmental and Geomatic Engineering, University College London, London, 2009.

Sun, X., Rosin, P. L., Martin, R. R, and Langbein, F. C.: Fast and effective feature-preserving mesh denoising, IEEE T. Vis. Comput. Gr., 925 - 938, doi: 10.1109/TVCG.2007.1045, 2007.

Suwandana, E., Kawamura, K., Sakuno, Y., Kustiyanto, E., and Raharjo, B.: Evaluation of ASTER GDEM 2 in comparison with GDEM 1, SRTM and topographic map derived DEM using inundation area analysis and RTK-d GPS data , Int. J. Remote Sens., 4, 2419-2431, doi:10.3390/ rs4082419, 2012.

Tran, T. A., Raghavan, V., Masumoto, S., and Yonezawa, G.: Enhancing quality of free DEM in Danang city, Vietnam and evaluating the suitability for terrain analysis, JSGI Geoinformatics, 24, 54-55, 2013a.

Tran, T. A., Raghavan, V., Yonezawa, G., Nonogaki., S., and Masumoto, S.: Enhancing quality of global DEMs for geomorphological analysis, case study in Danang city, Vietnam, 34th Asian Conference on Remote Sensing, Bali, Indonesia, 20-24 October 2013,. SC02.830-837, 2013b.

Yang, M. and Moon, W.M.: Decision level fusion of multi-frequency polarimetric SAR and optical data with Dempster Shafer evidence theory,in: IGRASS, 21-25July 2003, Toulouse, France, 2003.

Zandbergen, P.: Applications of shuttle radar topography mission elevation data, Geography Compass, 2, 1404-1431, 2008.

Zhao, S., Cheng, W., Zhou, C., Chen, X., Zhang, S., Zhow, Z., Liu, H. and Chai, H.: Accuracy assessment of the ASTER GDEM and SRTM3 DEM, an example in the Loess Plateau and North China Plain of China, Int. J. Remote Sens., 32, 1-13, doi:10.1080/ 01431161.2010.532176, 2011.

Table 1. General information of global DEMs and reference DEM (All the negative values were filled by neighboring pixels). Unit: m

	Min	Max	Mean	STD
GDEM	0	8016	271.8	319
SRTM	0	1634	277.5	304.6
Reference DEM	0	1664	268.1	302.6

Table 2. Results of GDEM after filling artifacts and shifting.

	RMSE (m)			Correlation
	Mountain	Flat	whole area	coefficient (R^2)
Original GDEM	91.2	4.2	75.6	0.9443
GDEM filled voids	17.8	4.2	14.9	0.9976
GDEM after shifting	15.4	4.1	13.0	0.9983

Table 3.SRTM before and after re-interpolation.

	RMSE (m)			Correlation
	Mountain	Flat	Whole area	coefficient (R^2)
Original SRTM	17.6	3.3	14.8	0.9979
Re-interpolated SRTM (30m)	15.0	3.2	12.6	0.9986

Table 4. The mean errors of GDEM and SRTM according to land cover map. Unit: m

	Agriculture	Forest	Built-up	Bare Land	Water
GDEM	0.7	1.0	1.1	-2.0	4.0
SRTM	1.9	6.3	2.5	3.8	0.4

Table 5. Mean of absolute error (MAE) from slope error maps of GDEM and SRTM on each landform area.

Landform class	GDEM (MAE)	SRTM (MAE)
Flat	2.1	1.6
Valley	5.8	5.7
Mountain Slope	6.08	6.1

Table 6. General statistics for the error of GDEM, SRTM and fused DEM. Unit: m

	Min error	Max error	MAE	RMSE
GDEM	-165.9	172.6	9.0	13.0
SRTM	-144.1	107	7.7	11.4
Fused DEM (before denoising)	-105.1	106.4	7.4	11.0
Fused DEM (after denoising)	-102.2	101.2	7.9	11.6

Table 7: Comparison of differences in some terrain parameters of GDEM, SRTM and Fused DEM with respect to Reference DEM

Attribute	**GDEM**	**SRTM**	**Fused DEM**
1. Slope			
-Mean of absolute error (MAE)	4.71	4.55	4.52
- STD of slope error	6.6	6.0	5.9
-Correlation Coefficient (R) to reference DEM	0.868	0.895	0.898
2. Profile curvature			
- MAE	0.0036	0.0027	0.0026
- STD	0.0054	0.0045	0.0044
- R	0.234	0.316	0.331
3. Tangential curvature			
- MAE	0.0043	0.0036	0.0035
- STD	0.0064	0.0059	0.0059
- R	0.271	0.326	0.322
4. Topographic Roughness Index			
- MAE	2.79	3.02	3.01
- STD	3.9	3.7	3.6
- R	0.71	0.75	0.76

Table 8: Result of angular difference of unit NVs between global DEMs, fused DEM and Reference DEM

Angular difference	GDEM	SRTM	FusedDEM
Min	0.0005	0.0015	0
Max	81.9	68.1	67.4
Mean	7.81	7.39	7.33
STD	6.85	7.03	7.06

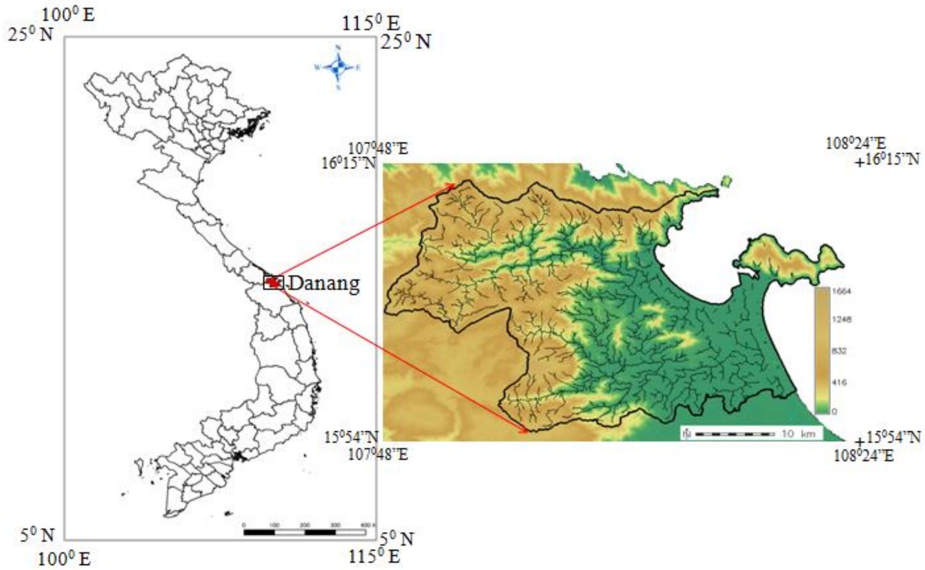

Fig. 1. Location of study area and topographic overview.

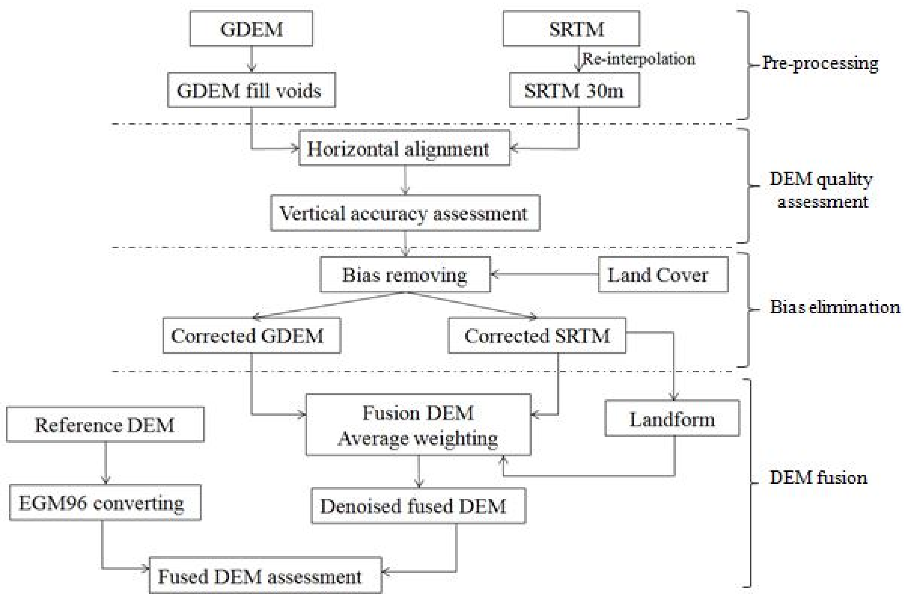

Fig. 2. Flowchart of data processing.

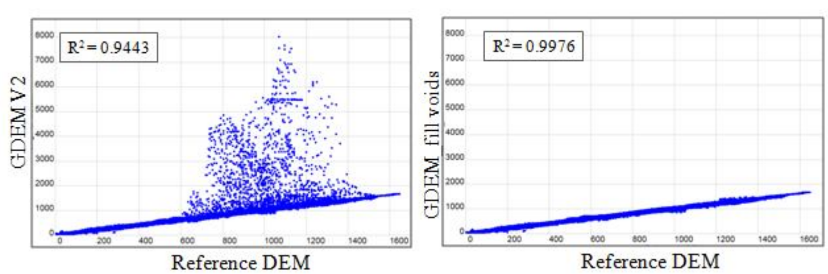

Fig. 3. Correlation between GDEM and Reference DEM before (left) and after (right) filling voids.

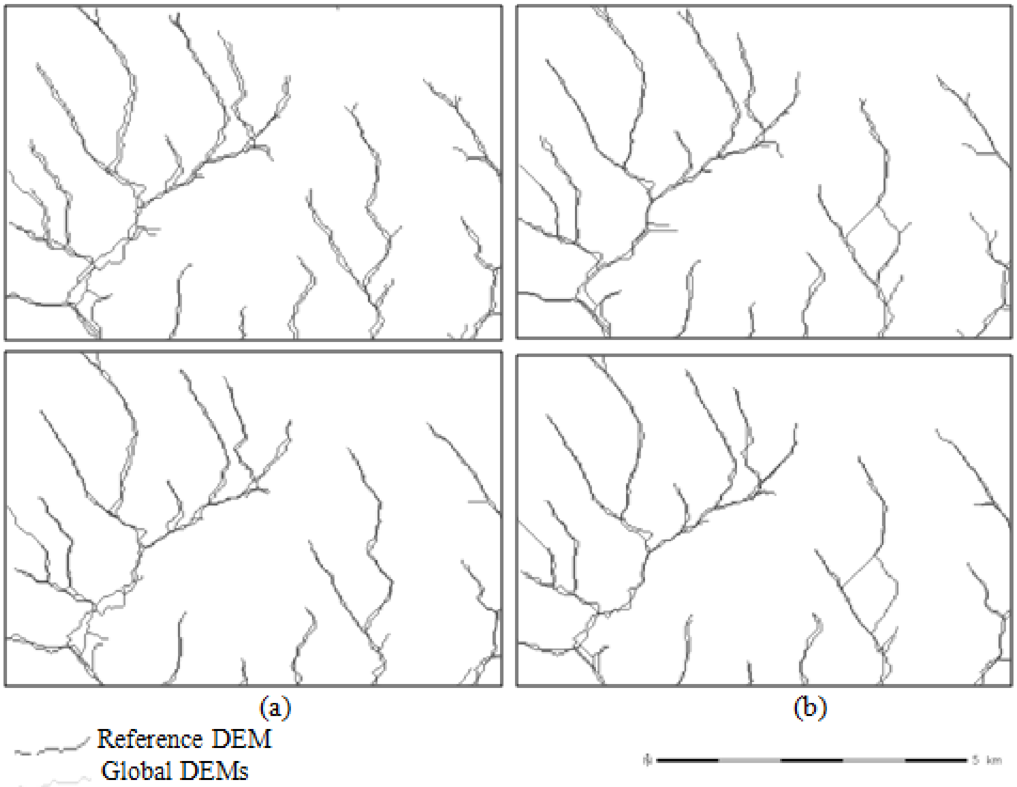

Fig. 4. Comparing stream networks of global DEMs and Reference DEM before (up) and after (down) shifting DEM: (a) GDEM; (b) SRTM.

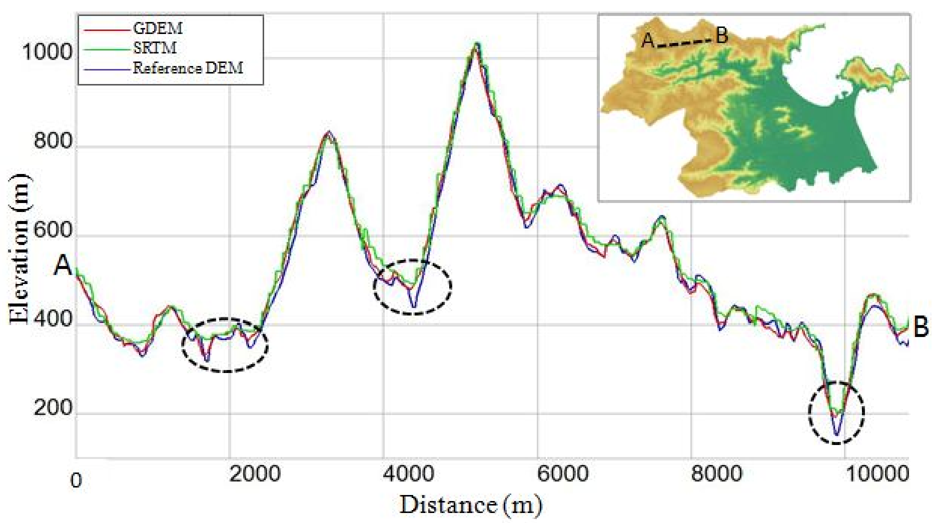

(a)

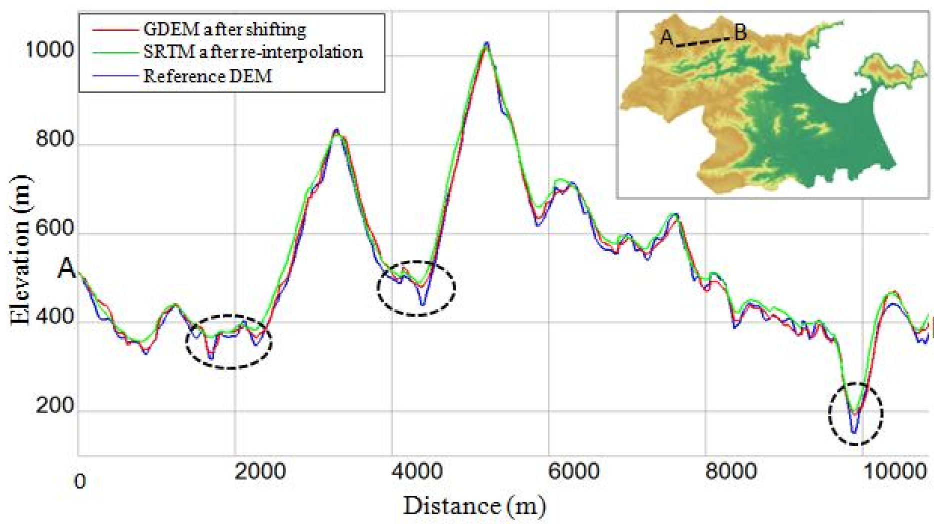

(b)

Fig. 5. Comparing GDEM and SRTM to Reference DEM: (a) before re-interpolation SRTM and shifting data; (b) after re-interpolation SRTM and shifting data.

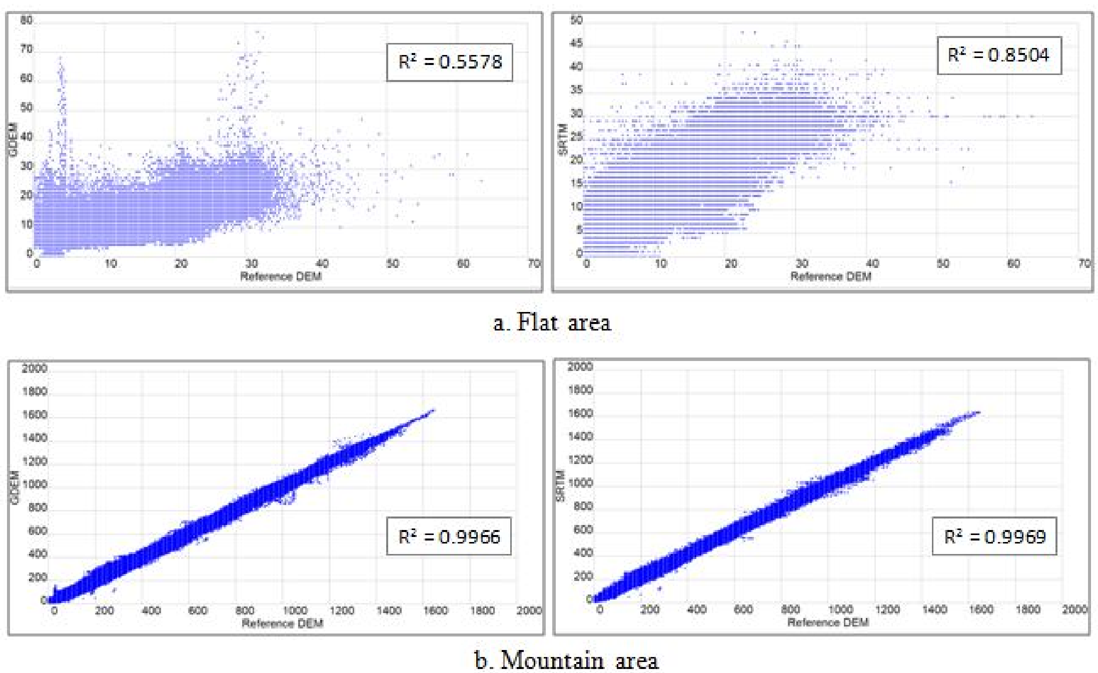

Fig. 6. Correlation of GDEM and SRTM in flat (a) and mountainous (b) area.

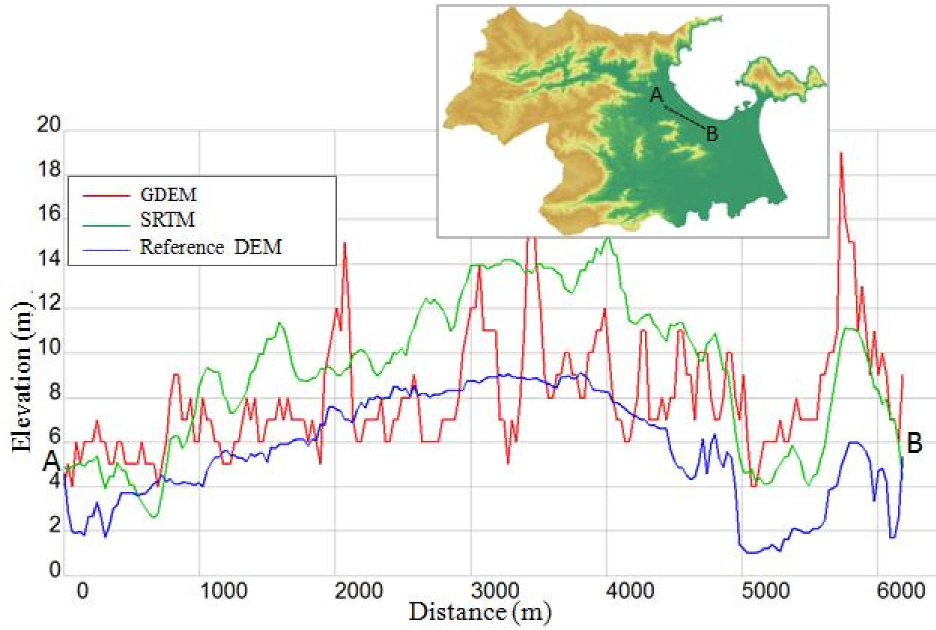

Fig. 7. A profile of GDEM and SRTM compare to Reference DEM in flat area.

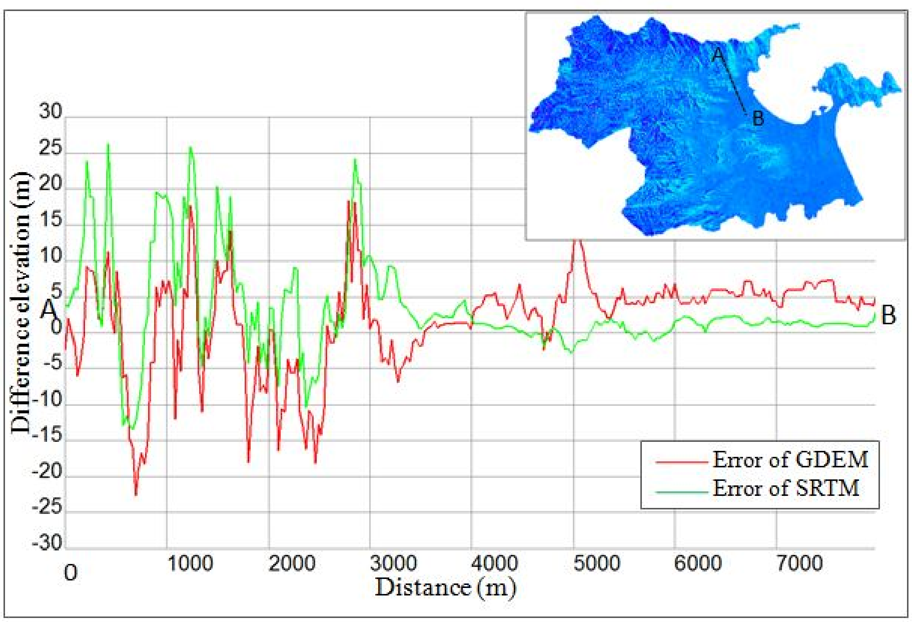

Fig. 8. Difference elevation of GDEM and SRTM with respect to Reference DEM from mountain to flat area.

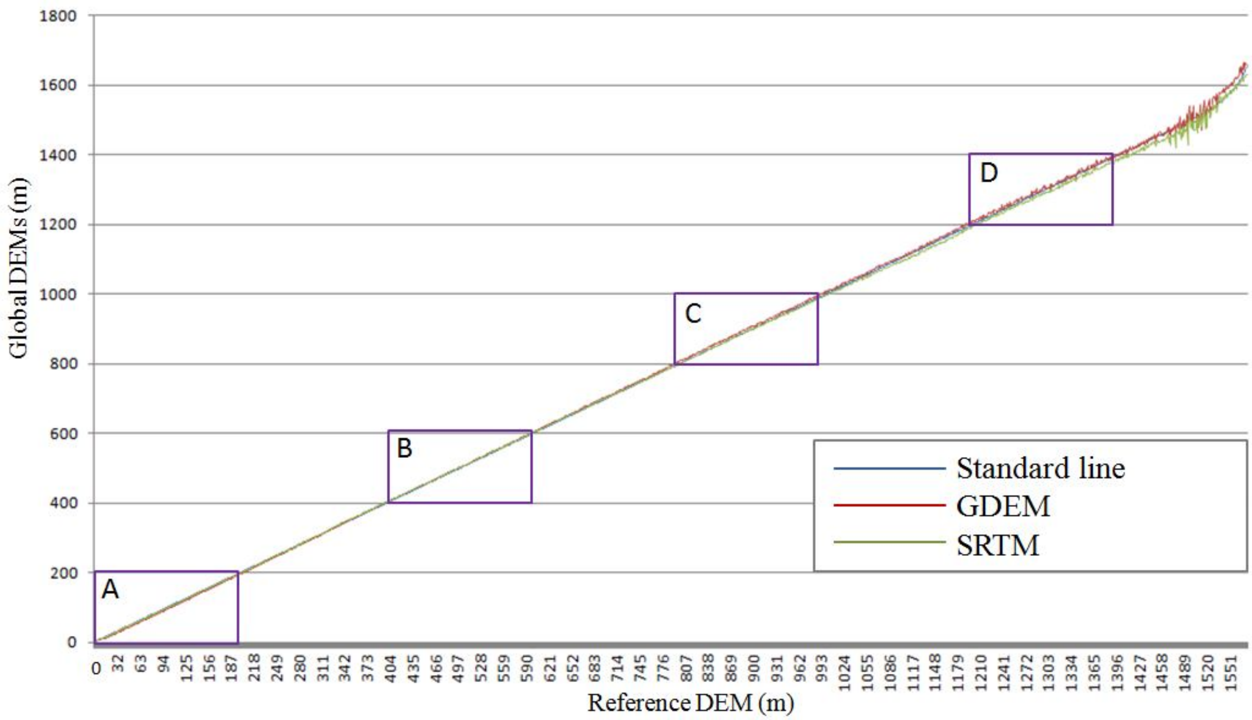

Global DEMs (m)
1800
1600
1400
1200
1000
800
600
400
200
0
A
B
C
D
Standard line
GDEM
SRTM
0 32 63 94 125 156 187 218 249 280 311 342 373 404 435 466 497 528 559 590 621 652 683 714 745 776 807 838 869 900 931 962 993 1024 1055 1086 1117 1148 1179 1210 1241 1272 1303 1334 1365 1396 1427 1458 1489 1520 1551
Reference DEM (m)

(a)

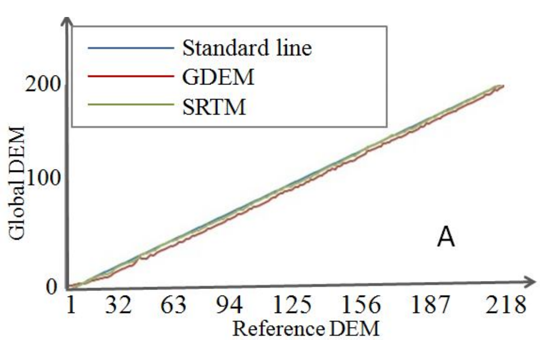

Standard line
GDEM
SRTM
Global DEM
200
100
0
A
1 32 63 94 125 156 187 218
Reference DEM

(b)

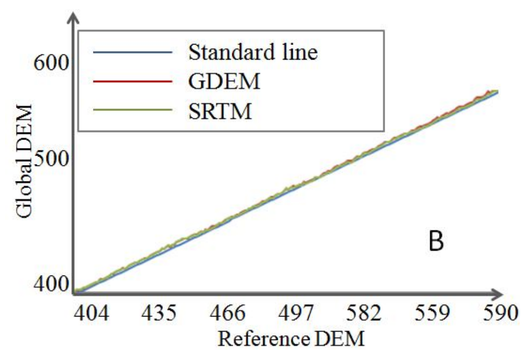

Standard line
GDEM
SRTM
Global DEM
600
500
400
B
404 435 466 497 582 559 590
Reference DEM

(c)

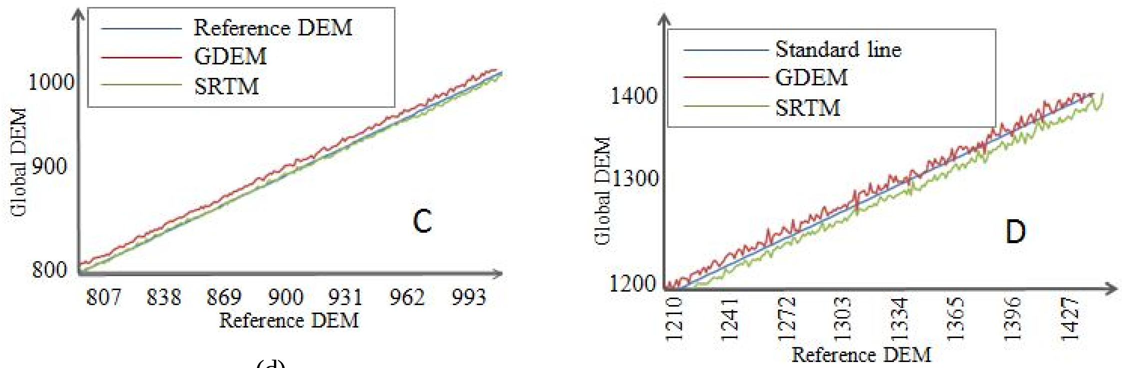

(d) (e)

Fig. 9. Behaviour of GDEM and SRTM to Reference DEM in difference topographic contexts.

(a)Whole area; (b)A area; (c) B area; (d) C area; (e) D area.

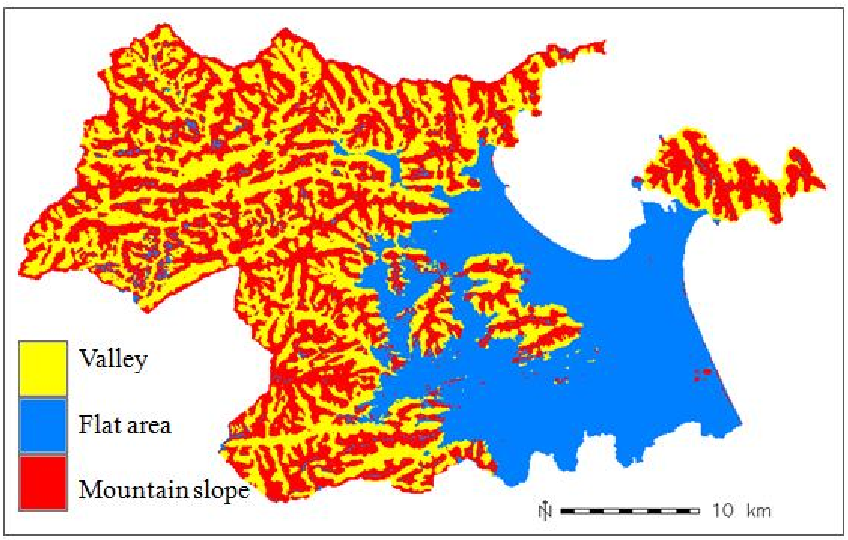

Fig. 10. Landform classification map from SRTM.

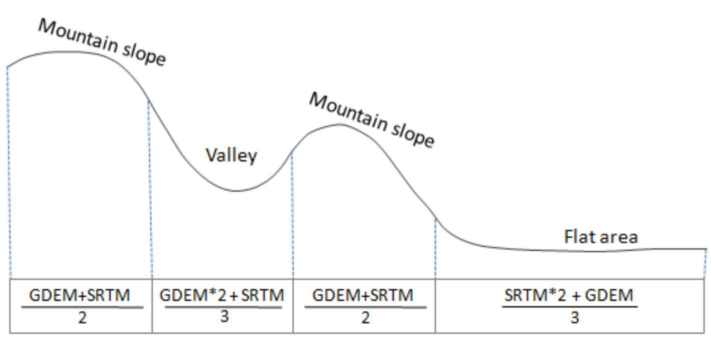

Fig. 11. Weighted averaging used to fused global DEMs.

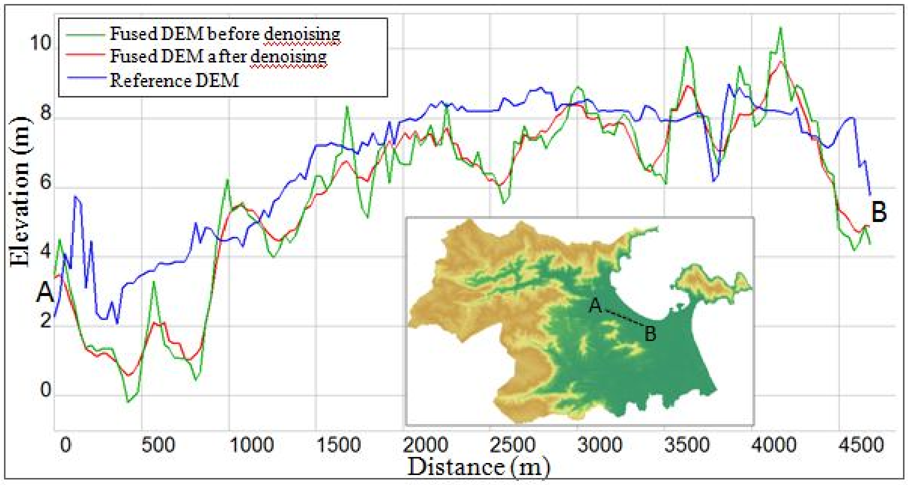

Fig. 12. Result of denoising algorithm (Sun *et al.* 2007) on fused DEM.

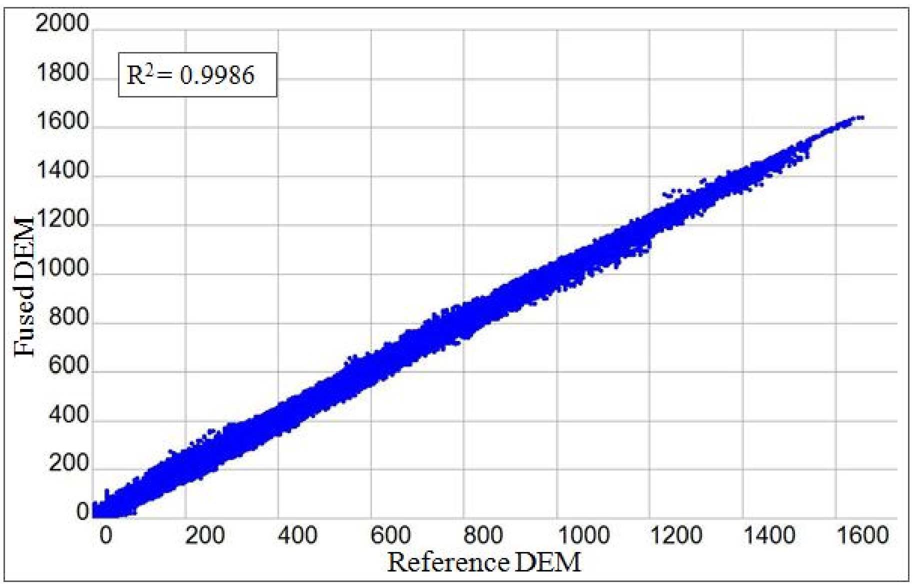

Fig. 13. Correlation between fused DEM and Reference DEM.

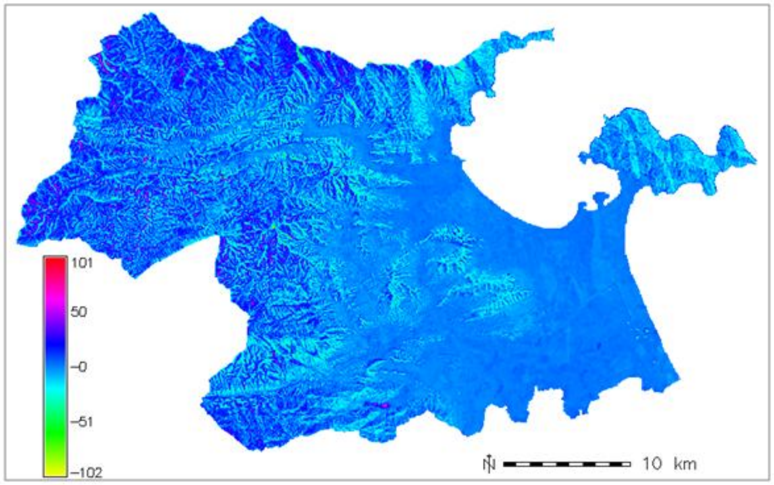

Fig. 14. Difference in elevation between fused DEM and Reference DEM.

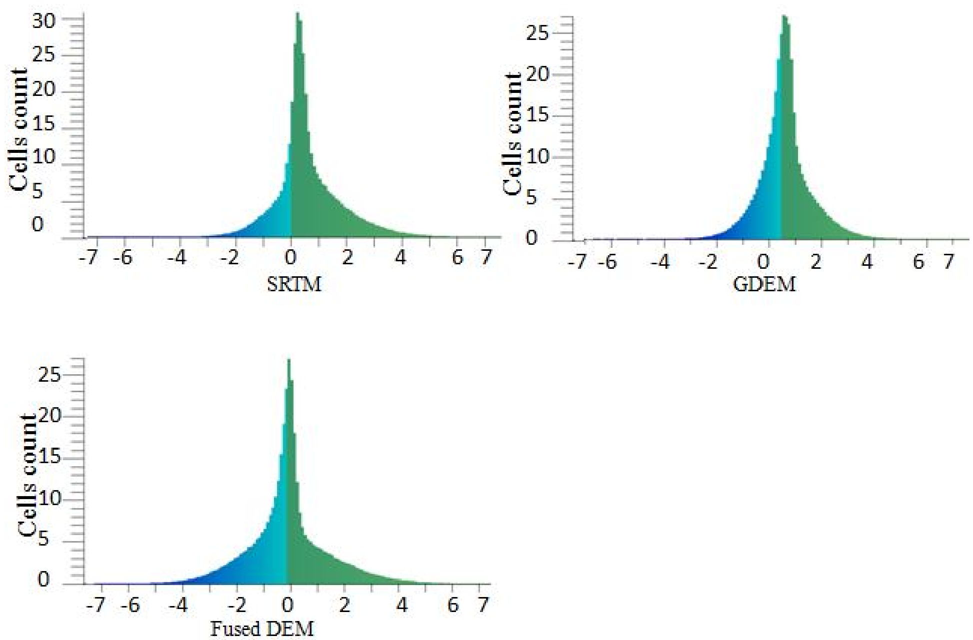

Fig. 15. Histogram from the difference elevation maps of SRTM, GDEM and Fused DEM. (X axis: cell values in tens; Y axis: number of cells in thousands)

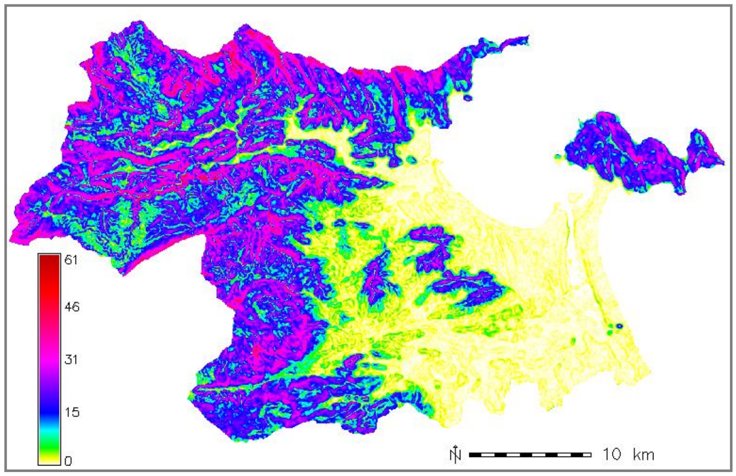

(a)

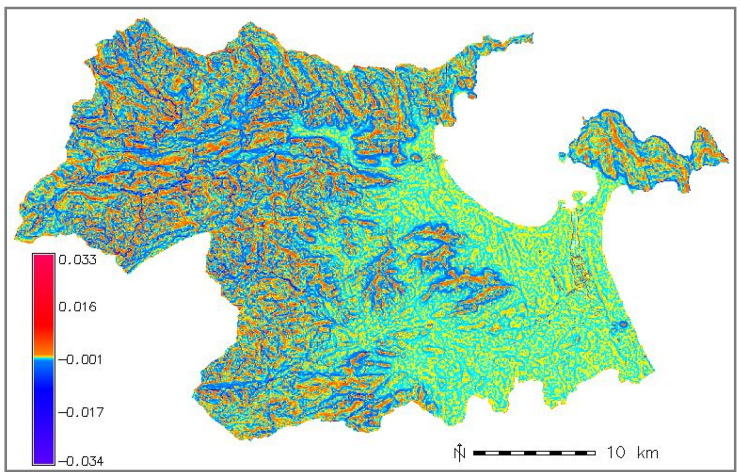

(b)

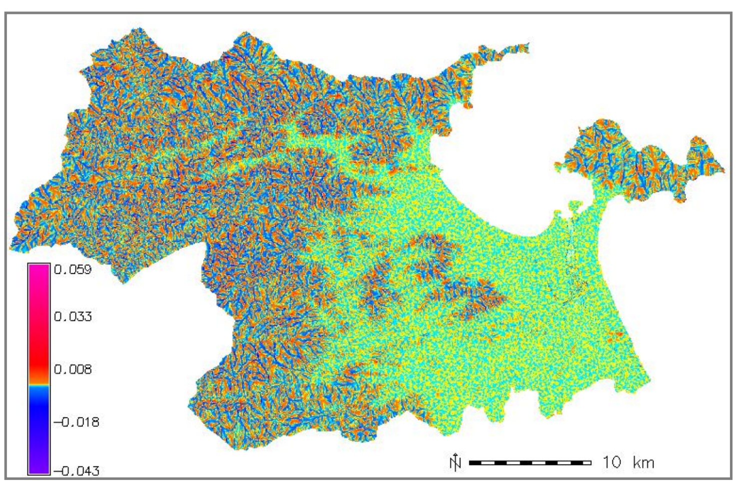

(c)

Fig. 16. Slope (a), Profile curvature (b) and Tangential curvature (c) maps extracted from Fused DEM.

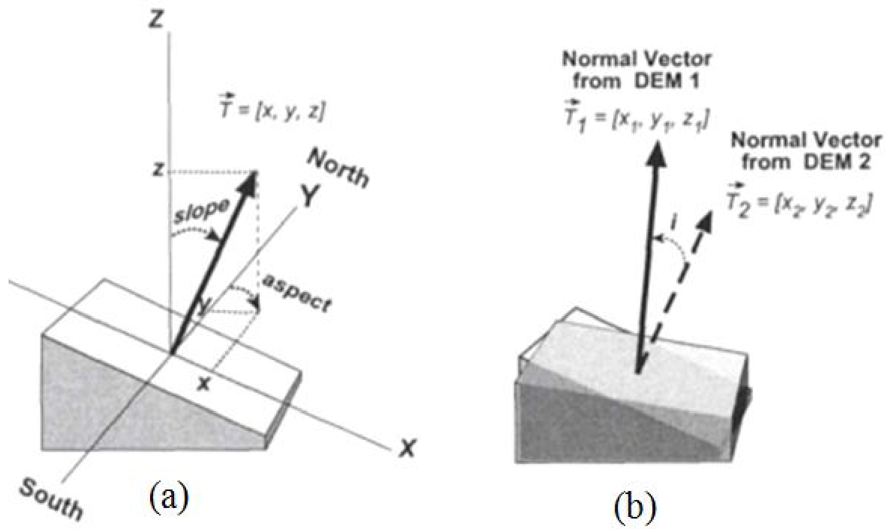

Fig. 17. Normal vector of a topographic surface (a) and the angular difference between two normal vectors (Hodgson and Gaile, 1999).